13.1 EFFECTS OF DIABATIC COOLING ON THE FORMATION OF CONVECTIVE SYSTEMS UPSTREAM OF THE APENNINES DURING MAP IOP-8

Heather Dawn Reeves *and Yuh-Lang Lin

North Carolina State University

Raleigh, NC

1. Introduction

An important focus of the Mesoscale Alpine Programme (MAP) is to better understand the dynamics of heavy precipitation events over the southern Alpine region (Bougeault et al. 2001). One event during MAP, IOP-8, was forecasted to have heavy precipitation and convection on the upslopes of the Alps. However, only light, stratiform precipitation fell in this area (Bousquet and Smull 2003). The lack of convection over the upslopes of the Alps has been attributed to the existence of a stable layer that extended over the Po Valley and south of the Ligurian Apennines (Medina and Houze 2003). Bousquet and Smull (2003) presented asynoptic data that shows convection did occur during IOP-8, but that it was over the Ligurian Sea, at the leading edge of the stable layer.

The synoptic environment of IOP-8 had many of the ingredients often present during heavy orographic precipitation events (Lin et al. 2001). Between October 20 and 21 1999 an eastward moving trough approached a quasi-stationary ridge over eastern Europe. Associated with the trough was a moderately strong low-level jet (LLJ) that advected high equivalent potential temperature (θ_e) air from over the Mediterranean Sea toward the southern Alpine region. The airstream impinging on the southern Alpine region was convectively unstable. Over the Po Valley and northern Ligurian Sea, there existed a cool, stable layer. Satellite and lightning imagery show that the leading edge of this stable layer was characterized by strong convection. This event was simulated using MM5 v3.5 (Dudhia 1993) in order to examine the effects of the cold, stable layer on a greater temporal and spatial resolution than the observed data allows.

2. MM5 experiments

The MM5 simulation was initialized using NCEP reanalysis data at 10/19/12Z and integrated for 60 hours. Three domains were used in this simulation with resolutions of 45, 15, and 5 km. All analyses presented herein come from the 15 km simulation. The Blackadar planetary boundary layer and Goddard-LFO (Tao and Simpson 1993) microphysical parameterization schemes were used in all domains. The Betts-Miller (Grell) cumulus parameterization scheme was used in the 45 km (15 and 5 km) domain(s). The MM5 simulation agrees well with the reanalysis data and observed data.

Figure 1 is a north-south cross section at 10/21/06Z of θ_e and wind vectors which show the incident airstream as being lifted over the stable layer. Above the stable layer is a convectively unstable layer. *We hypothesize that the stable layer behaved as an effective mountain over which the incident airstream was lifted as though being lifted over terrain and, furthermore, that the lifting by the effective mountain was sufficient for the release of convective instability.*

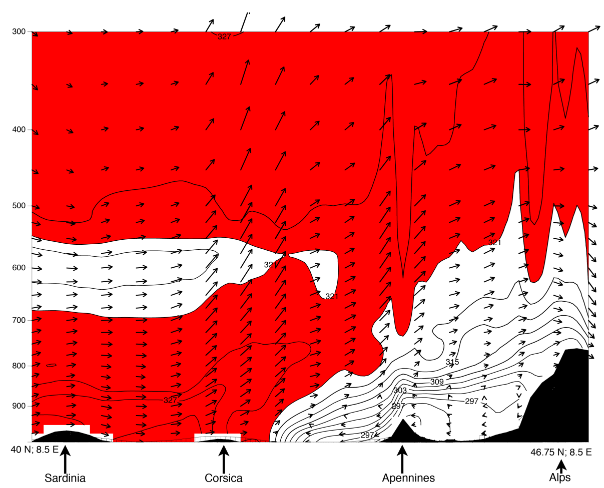

Figure 1: Cross section along line AB in Fig. 2 showing θ_e contoured every 3 K values greater than 321 K shaded and wind vectors at 10/21/06Z.

Lin et al. (2001) noted that the component of vertical motion due to orographic lifting is proportional

* *Corresponding author address:* Marine, Earth and Atmospheric Sciences North Carolina State University Box 8208 Raleigh, NC 27695-8208 email: hdreeves@unity.ncsu.edu

to the horizontal wind speed of the incident airstream (U) and the slope of the terrain ($\frac{\partial h}{\partial x}$) as follows:

$$w_{oro} = U\frac{\partial h}{\partial x} \quad . \tag{1}$$

Replacing $\frac{\partial h}{\partial x}$ in (1) by the slope of the effective mountain, which can be approximated by the $\theta_e = 310$ K isentrope, the vertical motion due to orographic lifting by the effective mountain (w_{eff}) was calculated. Figure 2 shows the height (in hPa) of the $\theta_e = 310$ K contour along with the effective mountain orographic moisture flux (given by $w_{eff}q$ where q is the mixing ratio) at 10/21/06Z and accumulated precipitation from 10/19/12Z to 10/21/12Z. Notice that the maxima in $w_{eff}q$, precipitation, and the leading edge of the effective mountain are nearly vertically aligned, each forming an arc over the Ligurian Sea. Further analysis of the total moisture flux (wq; not shown) reveals the effective mountain orographic moisture flux comprises a significant percentage of the total moisture flux which suggests lifting by the effective mountain was the primary source of convection over the Ligurian Sea.

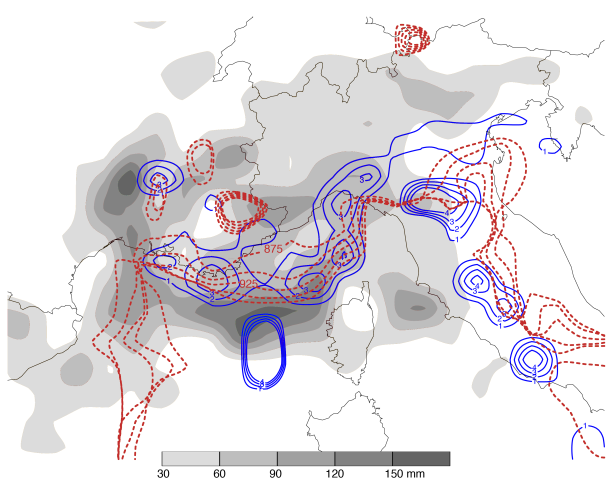

Figure 2: MM5 15 km simulation at 10/21/06Z showing effective mountain terrain (red, dashed, every 25 hPa), $w_{eff}q$ (10^{-4} m g kg^{-1} s^{-1}, blue contours), and accumulated precipitation (shaded as in legend) from 10/19/12Z to 10/21/12Z.

3. Idealized experiments

Idealized simulations were performed to better understand the effects of a stable layer on the location and intensity of convection. These experiments were performed using ARPS v5 (Xue et al. 200). This model solves the fully compressible, three-dimensional, nonhydrostatic equations in terrain following height coordinates ($\sigma - z$). Fourth and second order advection schemes were used in the horizontal and vertical directions, respectively. The horizontal grid spacing is 2 km with 512 grid points in the north-south direction. The vertical grid spacing is stretched from 40 m in the lowest 400 m of the domain to 370 m at the domain top. There are 120 vertical levels which give a domain height of 18 km. The boundary conditions in the east and west (north and south) directions were periodic (radiation). The lower boundary was free slip. A sponge layer was applied above 14 km to reduce artificial wave reflection by the upper boundary. In all simulations, the model time step is 3 seconds. Each simulation was integrated for 23 hours. Microphysical processes were handled using a parameterization scheme based on Lin et al. (1983).

The Alps and Apennines are represented by idealized two-dimensional mountain geometry given by

$$h = h_m \exp\left[-\left(\frac{y - y_0}{a}\right)^2\right] \quad , \tag{2}$$

where h is terrain height, h_m is the maximum terrain height (1 km for the Apennines and 2 km for the Alps), and a is the mountain half width (10 km for the Apennines and 30 km for the Alps). The peaks of the Apennines and Alps are 200 km apart. The mountains were introduced impulsively into the domain at time $t = 0$ s.

The effects of a cool, stable layer on the location and intensity of convection were examined through comparison of two simulations: a two mountain simulation, 2MTN, using the terrain described above and a second simulation identical to the 2MTN simulation only with prescribed cooling between the Alps and Apennines and south of the Apennines. The cooled layer had an initial temperature perturbation of -10 K at t = 0 s. Additional cooling at a rate of 34 K day^{-1} was applied to insure the stable layer remained in this location throughout the integration period. A certain adjustment time is expected given these initial conditions. However, this adjustment is not expected to be entirely unrealistic as the stable layer in the actual event was present several hours before southerly winds impinged upon it.

Each experiment was initialized using the 00 UTC 21 October 1999 (IOP-8) Cagliari sounding (Fig. 3) with a uniform southerly wind of 10 m s^{-1}. This sounding has a relatively low lifting condensation level (LCL) of 871 m which is lower than the height of the Apennines, therefore, condensation over the Apennines is expectable. The level of free convection (LFC) for this sounding is about 3000 m, implying that lifting by either the Apennines or the Alps is not sufficient for the release of conditional instability. The CAPE for the input sounding is 374 J kg^{-1}. Using the height of the Apennines, the moist Froude number (F_w; Chu and Lin 2000) far upstream of the mountain complex is 0.85 meaning the flow over the Apennines in the STBL and 2MTN cases is in flow regime IV of Chen and Lin (2004). This regime is characterized by a stationary stratiform system over the peak of the terrain. The sounding at y = 700 km and t = 20 h for the 2MTN simulation has an LFC of 1860 m, a CAPE of 310 J kg^{-1}, and a F_w of 0.47. This puts the flow over the Alps in the 2MTN simulation in flow regime II of Chen and Lin (2004) which is characterized by a stationary convective system over the peak of the terrain. Conversely, the sounding at y = 700 km in the STBL simulation is stable with $F_w = 0.32$, meaning convection is not favored in the STBL simulation.

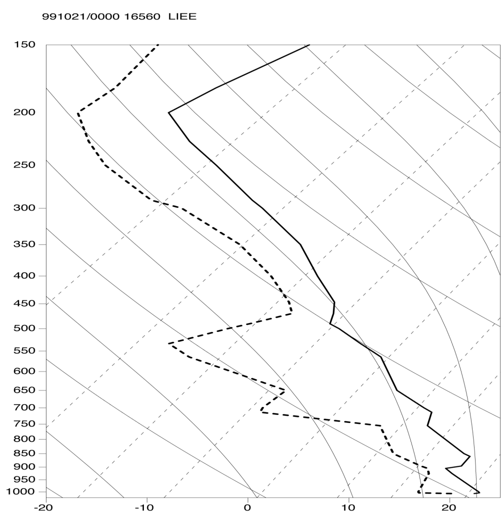

Figure 3: Sounding from Cagliari 10/21/00Z showing temperature (solid line) and dew point temperature (dashed line)

In the 2MTN simulation, there was a stationary convective system over the peak of the Alps as anticipated. This can be observed in Fig. 4 which shows a vertical cross section of θ_e and total water mixing ration q_w at t = 20 h. The stationary convection over the peak of the Alps was associated with a precipitation maximum in excess of 125 mm at y = 790 km. A stratiform cloud was present over the Apennines, as expected. However, no precipitation was generated by this cloud system.

Figure 5 shows a Hovmoller diagram of w at σ = 2.5 km for the STBL simulation. In this simulation, convection was initiated just upstream of the Alps at about t = 100 min. This convective system propagated upstream until it reached the leading edge of the stable layer at about t = 700 min. At which time, the convective system became stationary over

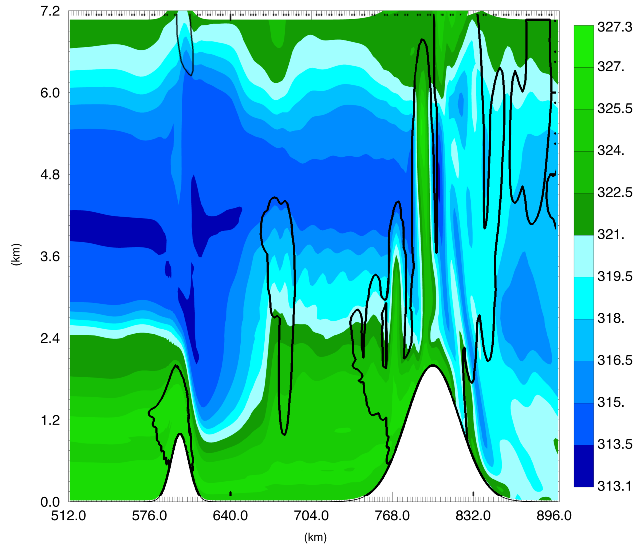

Figure 4: Cross section showing θ_e (shaded as in legend) and total water mixing ratio = 5 × 10^{-3} g kg^{-1} (contoured) for the 2MTN simulation.

the leading edge of the upslope of the effective mountain (about y = 500 km). The convection at the leading edge of the stable layer generated a precipitation maximum of about 40 mm at y = 550 km.

The presence of convection in the STBL simulation is not consistent with the F_w diagnostics or with parcel theory. However, the shape of the stable layer, because it is less steep than the slope of the Apennines, may be conducive to layer lifting and, as the LCL was low, layer destabilization and convection. This process appears to have happened. Figure 6 shows moist Brunt-Väisälä frequency (N_m^2) at t = 7 hrs for the STBL simulation. This time is just before the onset of convection. Notice there exists a layer of $N_m^2 < 0$ just above the effective mountain. There is also a shallow, saturated layer of moist absolutely unstable air at the base of this conditionally unstable layer.

The formation of convection upstream of the leading edge of the stable layer in the STBL simulation may be linked to the hydraulic jump to the lee of the Apennines. Figure 7 shows θ_e and q_{cld} at t=20 h for the STBL simulation. At this time, convection is located upstream of the Apennines. Also at this time, the hydraulic jump to the lee of the Apennines was advecting low θ_e air from midlevels downward such that the region just downstream of the Apennines was characterized by near moist-neutral conditions and a well-mixed environment. This well-mixed zone zone just to the lee of the Apennines may have acted as a quasi-rigid boundary along which impinging low-level, high θ_e air is forced upward leading to the de-

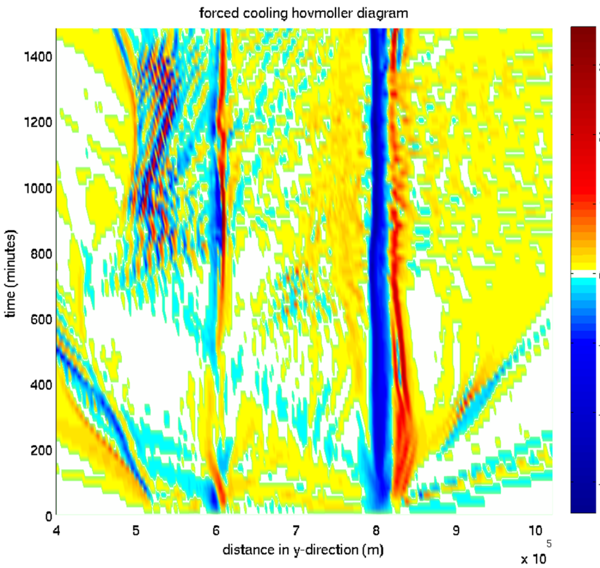

Figure 5: Hovmoller diagram of w (m/s; shaded as in figure) for the STBL simulation at $\sigma = 2.5$ km.

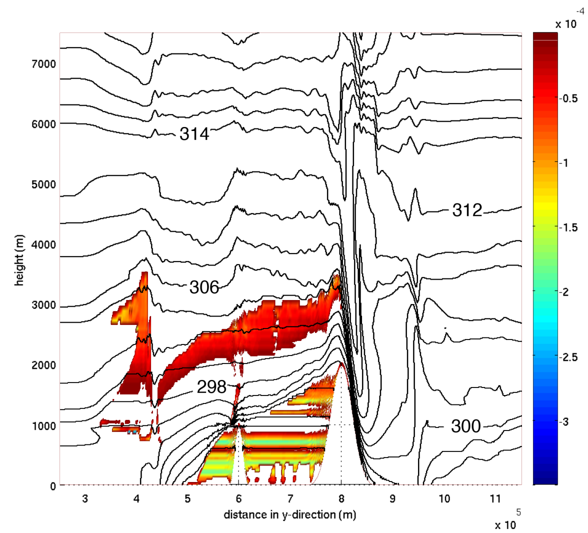

Figure 6: Cross section showing potential temperature (contoured) and N_m^2 (shaded as in legend) at blank hours for the STBL simulation.

velopment of convection upstream of the Apennines.

In order to test the notion that the stable layer behaved as an effective mountain, an additional simulation, called MMTN, was performed where the terrain was modified so that it was similar in shape to the θ_e = 312 K surface at t = 12 h, which is just prior to the development of convection upstream of the Apennines in the STBL simulation. Figure 8 shows θ_e and q_{cld} at t = 20 h for the MMTN simulation. At this time, the convection is contained between the peaks in the orography at y = 600 and 800 km. Although a hydraulic jump did form in this simulation, it was not strong enough for the dead zone to fully develop. Hence, the low-level, high θ_e air continued to be advected northward over the gentlest part of the slope where convection ensued. Above the leading edge of the modified mountain (between y = 500 and 600 km), the clouds are stratiform, not convective as in the STBL simulation. However, the convection between y = 600 and 800 km in the MMTN simulation appears to be the result of layer destabilization (not shown) as in the STBL simulation.

4. Conclusions

These simulations yield several significant findings.

- In the MM5 simulation, the stable layer appeared to behave as an effective mountain over which the incident airstream was lifted as though being lifted over terrain.
- Despite the fact that the orographic lifting was insufficient to release CAPE according to traditional parcel theory, convection was still able to develop in the STBL and MMTN simulations. This convection appears to be the result of layer destabilization.
- Convection upstream of the Apennines in the STBL simulation appears to be partly due to the downward advection of low θ_e air by the hydraulic jump which blocked the northward progression of high θ_e air.
- The MMTN simulation failed to produce convection at the leading edge of the modified mountain. This could either imply that the stable layer in the STBL simulation did not behave as an effective mountain or that the modified mountain did not accurately capture the shape of the effective mountain. It is possible that using some other parameters besides θ_e to design the shape of the modified mountain may yield more comparable results to the STBL simulation. It is also possible that the effective mountain in the STBL simulation may be better parameterized by a damping layer rather than rigid surface terrain.

Future work will extend beyond the IOP-8 case and attempt to diagnose the effects of upstream topography and extreme blocking for more idealized soundings with both convective and conditional instabilities.

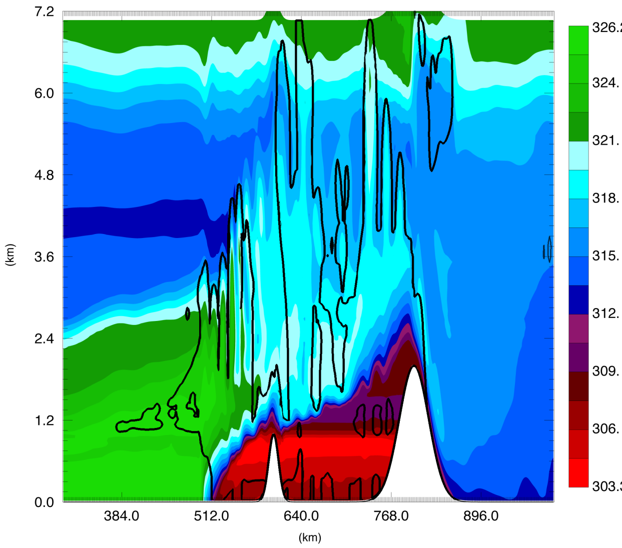

Figure 7: Cross section showing θ_e (shaded as in legend) and total water mixing ratio $= 5 \times 10^{-3}$ g kg^{-1} (contoured) for the STBL simulation.

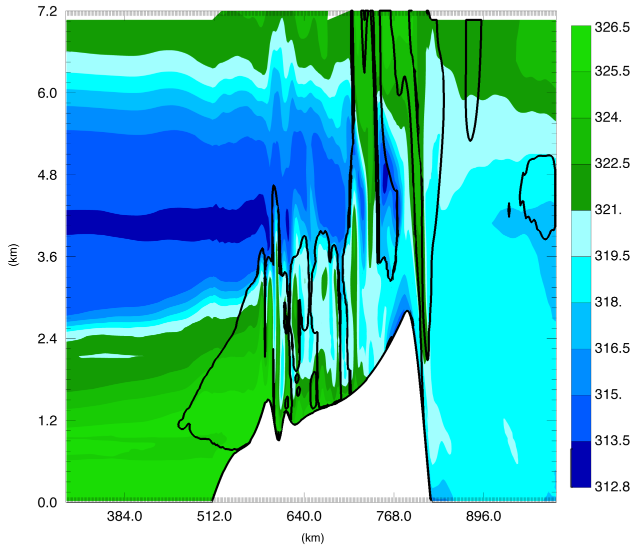

Figure 8: Cross section showing θ_e (shaded as in legend) and total water mixing ratio $= 5 \times 10^{-3}$ g kg^{-1} (contoured) for the MMTN simulation.

Acknowledgments

This research is supported by NSF Grants ATM-0096876 and ATM-0344237. Discussions with L. Carey, S. Medina, C. Schär, F. Semazzi, J. Stein, and the research results presented by other MAP colleagues are highly appreciated. Thanks to Ph. D. committee members M. Kaplan, J. Janowitz, and R. Rotunno.

References

Blackadar, A. K., 1979: High resolution models of the planetary boundary layer. *Adv. Environ. Sci. Eng.,* **1**, 50-85.

Bougeault, P., P. Binder, A. Buzzi, R. Dirke, R. Houze, J. Kuettner, R. B. Smith, R. Steinacker, and H. Volkert, 2001: The MAP special observing period. *Bull. Amer. Meteor. Soc.,* **82**, 433-462.

Bousquet, O., and B. F. Smull, 2003 (BS03): Observations and impacts of upstream blocking during a widespread orographic precipitation event. *Quart. J. Roy. Meteor. Soc.,* **129**, 391-410.

Chen, S.-H. and Y.-L. Lin, 2004: Effects of the basic wind speed and CAPE on flow regimes associated with a conditionally unstable flow over a mesoscale mountain. *Meteor. Atmos. Phy.*, in review.

Chu, C.-M., and Y.-L. Lin, 2000: Effects of orography on the generation and propagation of mesoscale convective systems in a two-dimensional conditionally unstable flow. *J. Atmos. Sci.,* **57**, 3817-3837.

Dudhia, J., 1993: A nonhydrostatic version of the Penn State-NCAR Mesoscale Model: Validation tests and simulation of an Atlantic cyclone and cold front. *Mon. Wea. Rev.*, **121**, 1493-1513.

Lin, Y.-L., R. D. Farley, and H. D. Orville, 1983: Bulk parameterization of the snow field in a cloud model. *J. Climate and Appl. Meteor.,* **22**, 40-63.

——, S. Chiao, T.-A. Wang, M. L. Kaplan, and R. P. Weglarz, 2001: Some common ingredients for heavy orographic rainfall and their potential application for prediction. *Wea. Forecasting,* **16**, 633-660.

Medina, S., and R. A. Houze, 2003: Air motions and precipitation growth in Alpine storms. *Quart. J. Roy. Meteor. Soc.,* **129**, 345-372.

Rotunno, R., and R. Ferretti, 2003: Orographic effects on rainfall in MAP cases IOP2B and IOP8. *Quart. J. Roy. Meteor. Soc.,* **129**, 373-390.

Tao, W.-K., and J. Simpson, 1993: Goddard Cumulus Ensemble Model. Part I. *Terr. Atmos. Ocean,* **4**, 35-72.

Xue, M. , K. K. Droegemeier, V. Wong, A. Shapiro, K. Brewster, F. Carr, D. Weber, Y. Liu, and D.-H. Wang, 2001: The advanced regional prediction system (ARPS) - A multiscale nonhydrostatic atmospheric simulation and prediction tool. Part II: Model physics and applications. *Meteor. Atmos. Phys.*, **76**, 134-165.